Study of Interaction of Short Fatigue Cracks in 2024T351 Aluminium Alloy

H. Proudhon[1] and J-Y. Buffière[1]

[1] GEMPPM (INSA de Lyon), CNRS UMR 5510, 20 Avenue Albert Einstein 69621 Villeurbanne Cedex.
Henry.proudhon@insa-lyon.fr
Jean-yves.buffiere@insa-lyon.fr

***ABSTRACT.** In the present paper, the growth of short fatigue cracks in center hole samples of a 2024T351 Aluminium alloy used in aerospace applications. Constant stress amplitude fatigue tests were carried out and the crack growth has been monitored by optical microscopy. were done. It is shown that three different type of cracks can be distinguished, according to their propagation behaviour. Those different behaviours have been studied with the EBSD (Electron Back Scatter Diffraction) technique. First results obtained show that crack growth is strongly influenced by the local crystallographic orientation even within the plastic zone arond the hole. Crack path prediction is succesfully implemented but the model still limits the predictions .*

INTRODUCTION

Fatigue of riveted lap joints has been the subject of many studies because of its importance in aeronautical design. Industrial work [1] shows that fatigue prediction of such joints, could be improved by taking into account the very first millimeters of the crack growth, i.e. when the cracks fall in the short cracks regime.

It is now well known that such short fatigue cracks strongly interact with the microstructure. Moreover, another important difficulty for the observation of short cracks is the three dimensional aspect of the propagation behaviour, wich cannot be observed without using X ray tomography [2]. If crack closure is also considered, this result in a quite complicated problem that is still not completely understood and even less predictable.

In this work, we try to correlate experimental short fatigue crack growth data, obtained in center hole samples which was not cycled to failure, with EBSD (Electron Back Scatter Diffraction) measurement around the crack to show and quantify the interaction of the fatigue cracks with the local microstructure.

EXPERIMENTAL METHODS

The material used in this work was a 2024 Aluminium alloy with T351 heat treatment. This material was supplied in rolled plates of 25mm thickness. Standard Fatigue hole notched samples were spark cut from the plates, in the center of the S (short transverse) direction to lower the possibility of material properties dispersion (see Fig. 1). No chamfer was machined at the hole edge in order to be able to observe cracks just after initiation by optical microscopy.
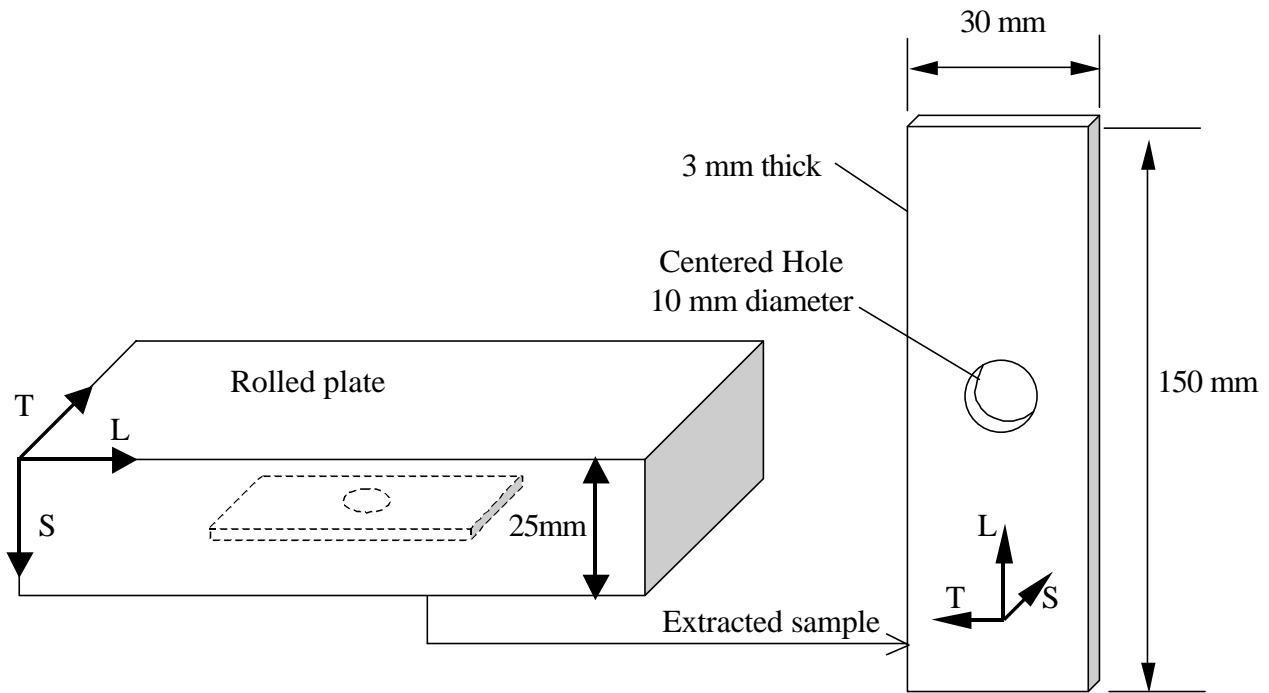

Figure 1. Fatigue sample extraction and geometry.

The two surfaces of each sample were mechanically polished using diamond paste down to 1 µm particle-size. Special care was taken to avoid "smoothing" at the holes edge during polishing.

All the specimens were loaded in the L direction at constant stress amplitude σmax=200 MPa in the hole section with a stress ratio of 0.1. During cycling, the specimen is dismounted every 1000 cycles and optically observed to detect crack initiation and propagation. A x100 magnification is used so that the initiation corresponds to the detection of a crack with a size of a few microns. For each studied crack, a(N) curves giving the crack length as a function of number of cycles have been plotted. Four samples (named 1,2,3 and 4 afterward) were cycled and 28 cracks have been studied. The cycling was stopped before failure in order to process EBSD measurement in zones submitted to cracking.

RESULTS OF THE FATIGUE TESTS

As expected, cracks initiate near the maximum loading location, at the hole edge and propagates in a direction wich is, globally perpendicular to the loading axis. We do not discuss initiation here focus on propagation. From the a(N) curves shown on Fig. 2 for samples 3 and 4, one can distinguish 3 types of propagations according to crack growth rate. Type 1 cracks nucleate, start to propagate and then stop with a typical crack length of 100 µm. Type 2 cracks still propagate at the end of the fatigue test but crack growth rate remains moderated ; these cracks never reach a 1mm size. Type 3 cracks propagates much faster than types 1 and 2 and would grow up to failure (see Table 1 for general information on fatigue tests). A Similar behaviour was observed for samples 1 and 2.

Table 1. General informations on fatigue tests.

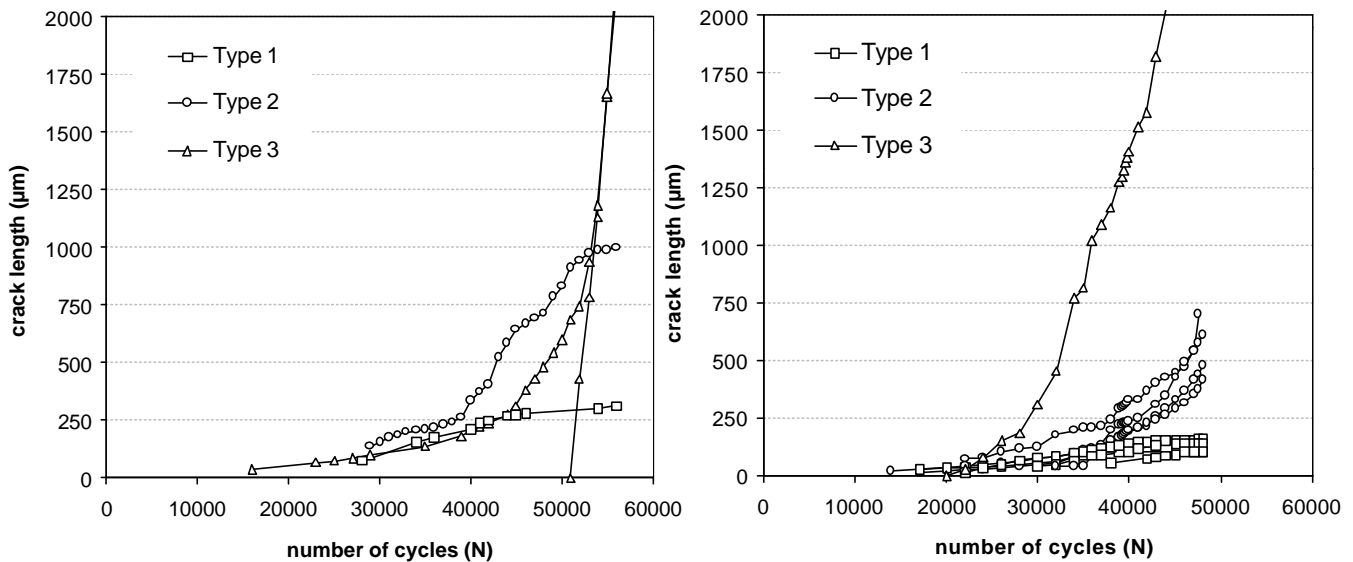| Specimen	No. of cycles	No. of cracks	stopped cracks (T1)	propagating cracks (T2 and T3)
1	40000	7	5	2
2	40000	8	4	4
3	56000	4	1	3
4	48000	9	4	5

Figure 2. Crack length optically measured versus number of cycles for samples 3 and 4.

The different types of propagation behaviour cannot be correlated with the angle of the crack with respect to the maximum stress plane in the sample (perpendicular to σ). Instead we do beleive that the different propagation behaviour can be accounted for by the interactions of the crack with the local microstructure. Indeed, as can be seen on Fig.3, optical inspections of the crack path reveal numerous interaction : deviations with deviation angles as large as 110°, grain boundary arrests or slow down, very straight propagation often parallel to slip bands. Such interactions are likely to strongly influence the local propagation rate of the cracks.
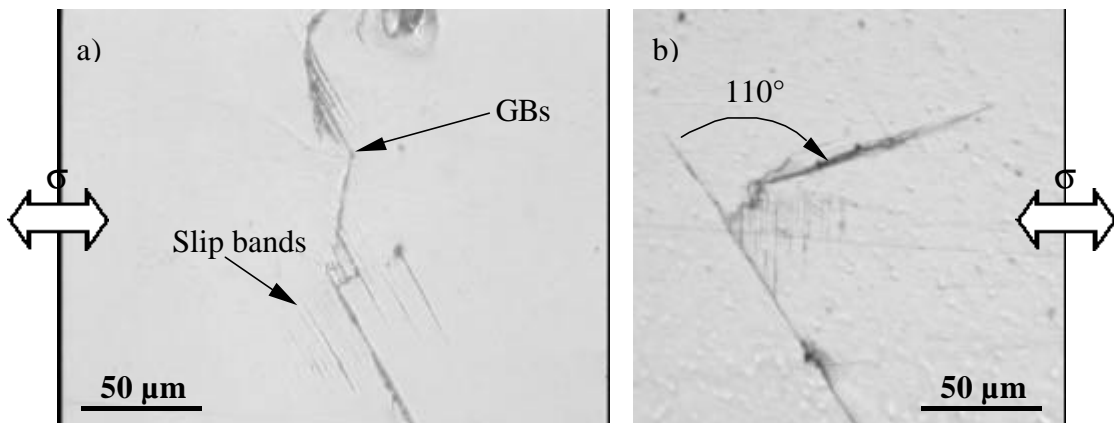

Figure 3. Crack deviations at grain boundaries in a 2024T351 alloy cycled at constant stress amplitude in a center hole sample (distance from the hole edge is 1.5 mm in picture a and 0.5 mm in picture b).
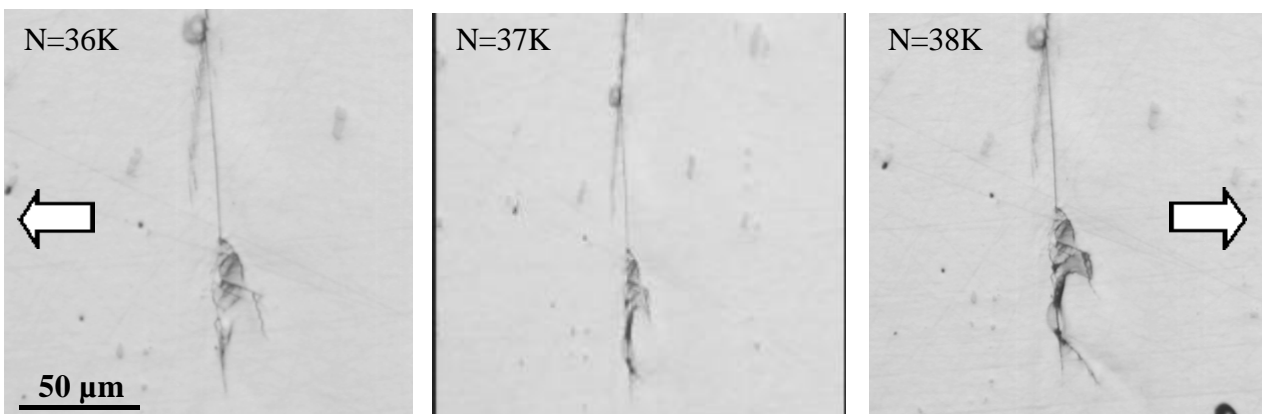

Figure 4. Crack arrest of 2000 cycles at a grain boundary in a 2024T351 alloy cycled at constant stress amplitude in a center hole sample (distance from the hole edge is 0.7 mm).
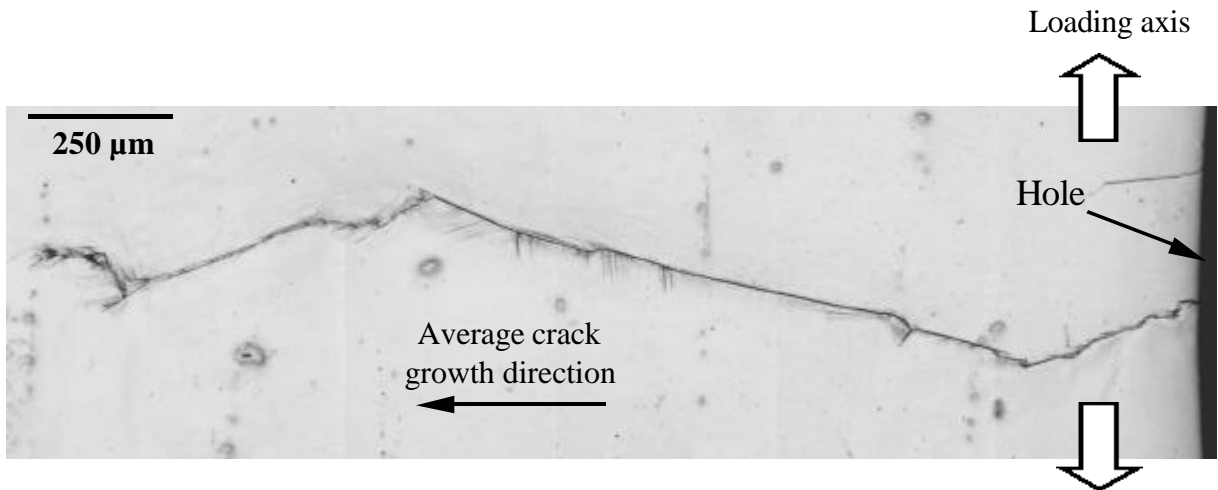
Figure 5. A typical crack of type 3 showing deviations, slip bands, and straigtht propagations. Specimen 3, crack A, 56000 cycles.

INFLUENCE OF THE LOCAL MICROSTRUCTURE ON CRACK PATH

Zhai and al. [3] have shown in an Al-Li alloy that a key parameter for the local crack path when a grain boundary is encountered is the twist angle α of the crack planes before and after the boundary (see Fig. 6). In order to check this mechanism for the 2024 alloy, Schmid factor, twist angles (α) and disorientations angles at grain boundaries (θ) have been measured from the EBSD data. Since our alloy present a microstructure with pancake/disc grain shapes due to rolling, we have assume (like Zhai and al.) that the crack meets grain boundaries parallel to the (L,S) plane as described in Fig. 6.
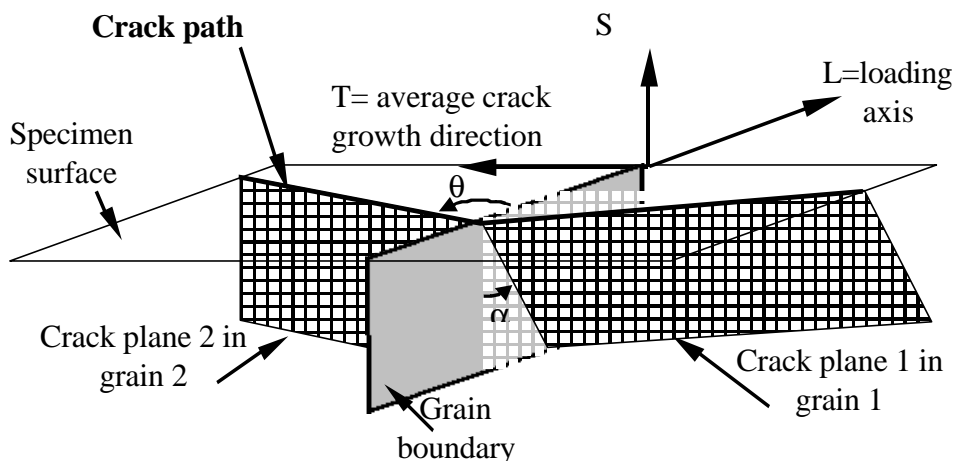

Figure 6. Definition of the twist angle α as the misorientation of the crack planes when a grain boudary is encountered.

The local crystallographic structure around cracks was studied by EBSD (see for example [4] for a rewiew of this technique and [5] for its implementation with cracked surfaces) in a scanning electron microscope JEOL 840A LGS fitted with a tungsten filament, a CCD camera, and the 'CHANNEL' softwear from HKL technology for the automatic acquisition and indexation of Kikuchi patterns. Orientation data have been analyses with home build calculations. All the fatigue specimens were cut to be handled more easily . The EBSD a technique being very sensitive to dislocation in the material, a thin layer (max 10 µm) hardened by mechanical polishing, was electrolitically removed. A new optical micrography of the surface crack shape is then taken and compared to the former one to ensure good preparation and that no major change has happened in the crack shape.

A typical example of EBSD acquisition around the crack path is presented in Fig. 7. The elongated grain shape and grain boundaries almost parallel to L axis can clearly be observed on that figure. The corresponding optical micrography after electropolishing has been superimposed on the EBSD map. This was done by taking a secondary electron image after EBSD acquisition. As each acquisition point in EBSD mode leave a mark on the surface visible in SEI mode, by comparison between the three images, the EBSD map and the optical micrography of the crack can be positioned very precisely.
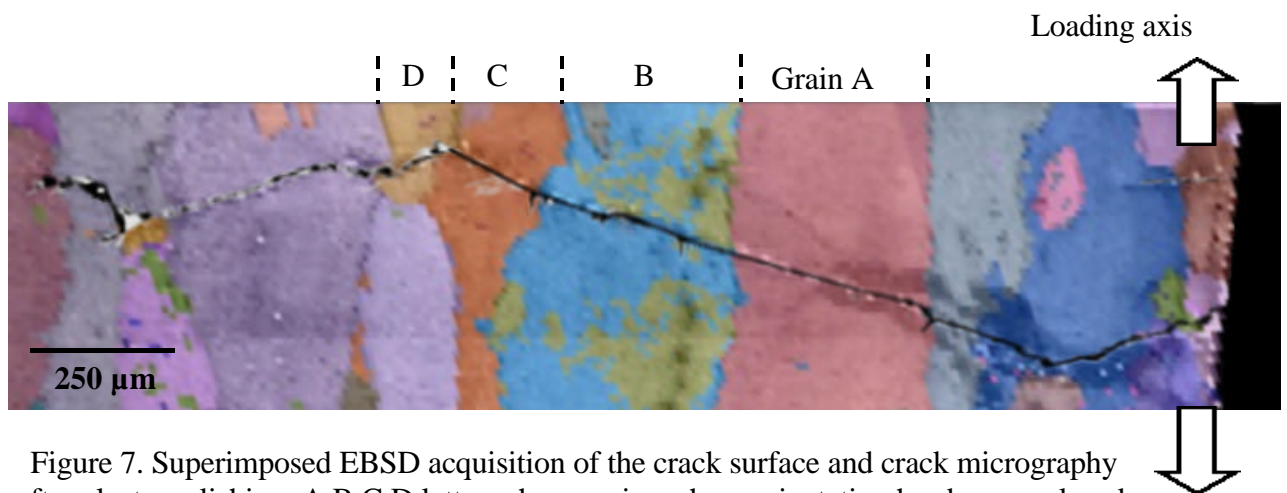

Figure 7. Superimposed EBSD acquisition of the crack surface and crack micrography after electropolishing, A B C D letters show grains where orientation has been analysed.

The results of the analysis on grains A, B ,C and D (defined on Fig. 8), are summarised in Table 8. from this table, it can be seen that in grains B and C, the crack is found to propagate on planes wich exhibit high schmid factors and wich also minimise the twist angle,within an accuracy of 5°. Slip bands corresponding to different slip planes with high Schmid factors are also observed but the crack propagates on the plane with the lowest value of α.

Table 2. Crystallographic orientations on grains A, B, C and D.

Grain	Orientation matrix			Slip planes	Predicted θ (°)	Observed θ (°)	Observed slip bands	Schmid factor	Predicted α (°)
grain A	0,92877	-0,17402	-0,32728	111	89,1	80	88	0,494	
	-0,0126	0,8676	-0,4971	-111	42,0			0,303	
	0,37045	0,46581	0,80361	1-11	-53,4			0,491	
				11-1	18,5			0,289	
grain B	-0,98973	0,06073	0,12939	111	27,8			0,372	67,8
	0,04522	-0,72573	0,68649	-111	-42,6	-45		0,451	64,3
	0,1356	0,68529	0,71553	1-11	80,0	76		0,413	10,7
				11-1	84,7		90	0,456	120,6
grain C	0,97879	0,09856	-0,17962	111	-84,2		-76	0,422	117,6
	-0,18265	0,81694	-0,54704	-111	67,2	66		0,468	8,3
	0,09283	0,56824	0,81761	1-11	-46,6			0,454	51,7
				11-1	24,5			0,333	84,8
grain D	0,31749	0,66543	-0,67557	111	-80,1	-60		0,260	22,7
	-0,94091	0,3096	-0,13723	-111	42,1	0		0,493	34,5
	0,11785	0,67922	0,72441	1-11	-82,3			0,462	87,2
				11-1	-25,7			0,381	28,5

In grain A, the 10° difference observed between predicted and observed θ angles is quite higher than the 5° accuracy previously assumed. One explanation may be that the crack path correspond to a combination of two slip planes (the one at 89° and another one). The observation of steps along the crack path (Fig. 8) is in support of this asumption.
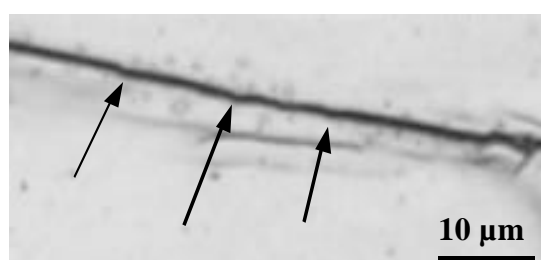

Figure 8. Optical micrography of the local crack path in grain A showing small steps (indicated by arrows) along the propagation plane.

In grain D, no correlation has been found between the crack path and the local activated slip planes and the local crack path looks highly tortuous (Fig. 8). This may be

explained by the little size of the grain crossed by the crack. The grain boundaries proximity is likely to disturb the activated slip system as shown by Parisot and al [6].

CONCLUSIONS AND FUTURE WORK

Fatigue tests in center hole samples show clearly different types of crack propagation wich cannot be linked to the local loading conditions, but rather to the interaction of the cracks with microstructure.

EBSD measurements around the crack path was performed. A crystallographic short crack propagation mechanism has been tested. Good agreement for prediction of crack plane propagation is found in some grains, and other activated slip systems visible can be predicted too. However no correlation is found when crack crosses a small grain, and in that case the crack path seems no longer crystallographic.

Further EBSD measurement are being carried out to provide statistical information on correlated/uncorrelated crack plane propagation in the 2024 alloy.

REFERENCES

1. Journet, B., Congourdeau, F. and Ithurralde (2003) Prevision de la fissuration par fatigue des alesages de jonctions rivetees. In : *Colloque National de Mecamat 2003 Aussois, France*, pp.129-136.
2. Buffiere, J-Y., Habilitation à diriger des recherches. INSA Lyon, 2002.
3. Zhai, T., Wilkinson, A. J. and Martin, J. W. (2000) A crystallographic mechanism for fatigue crack propagation through grain boundaries. *Acta Materialia* **48**, 4917-4927.
4. Schwarzer, R.A. (1997) *Micron* **28**, 249-265.
5. Gourgues, A-F. (2002) Electron backscatter diffraction and cracking. *Material Science and Technology* **18**, 119-133.
6. Parisot, R. et al. (2000) Modeling the mechanical behaviour of a multicrystalline zinc coating on a hot-dip galvanised steel sheet. *Computational Material Science* **19**, 189-204.